Available online at www.sciencedirect.com
SCIENCE DIRECT®
Polymer 44 (2003) 5737–5747
polymer
www.elsevier.com/locate/polymer

Three-dimensional phase morphologies in HDPE/EVA blends obtained via dynamic injection packing molding

Bing Na, Qin Zhang, Yong Wang, Rongni Du, Qiang Fu*

Department of Polymer Science and Materials, State Key Laboratory of Polymer Materials Engineering, Sichuan University, Chengdu 610065, People's Republic of China

Received 27 January 2003; received in revised form 7 May 2003; accepted 6 June 2003

Abstract

The formation of phase morphology of injection molded HDPE/EVA blends, under the effect of shear stress, has been investigated in detail. The shear stress was induced by dynamic packing injection molding, by which a specimen is forced to move repeatedly in the model by two pistons that move reversibly with the same frequency during cooling. Two kinds of EVA with VA content 16 wt% (16EVA) and 33 wt% (33EVA) were used to investigate the effect of interfacial tension. The phase morphology was viewed both parallel and perpendicular to the shear flow direction, so one can get an overall three-dimensional phase morphology. Low shear stress provided by the pistons has a substantial effect on the phase morphology along the flow direction but is insignificant in the direction perpendicular to the flow direction. Generally, a much elongated and layer-like structure is formed along the flow direction, and spherical droplet-like morphology is formed perpendicular to the flow direction, and the degree of deformation of rubber particles also depends upon their size and elasticity as well as on the interfacial properties between matrix and dispersed phase. For static samples of HDPE/16EVA blends (without shearing), only droplet morphology is formed as 16EVA content increases from10 to 40 wt%. However, under the effect of shear stress (dynamic samples), both droplet and cylinder morphologies can be formed depending on the volume ratio. For static samples of HDPE/33EVA blends, not only droplet, but also cylinder and co-continuous morphology (perpendicular to flow direction) can be formed depending on the volume ratio. For dynamic samples of HDPE/33EVA blends, droplet, cylinder and co-continuous network (co-continuous in both parallel and perpendicular to flow direction) can be formed under the effect of shear stress. The formation of phase morphology is discussed based on interfacial interaction, viscosity ratio, shear stress, and phase inversion.
Published by Elsevier Ltd.

Keywords: Phase morphology; Shear stress; Elongated particles

1. Introduction

One of the key factors, to achieve desired final properties is the controlling of the phase morphology. The morphology resulting from blending and processing depends mainly on the rheological and interfacial properties, the blending conditions, and the volume ratio of the components [1–5]. During processing, the morphological evolution in polymer blends is related to mechanisms such as elongated drop disintegration, minor phase relaxation, and coarsening [6–8]. The size and the deformation of a purely viscous (Newtonian) droplet surrounded by another Newtonian fluid is determined mainly by two parameters [9–11]: (1) the phase viscosity ratio (λ)

$$\lambda = \frac{\eta_d}{\eta_m} \tag{1}$$

where η_d and η_m are the viscosities of the dispersed and matrix, respectively, and (2) the k-term of the form

$$k = \frac{\sigma}{\eta_m \dot{\gamma} R} \tag{2}$$

where σ, interfacial tension, $\dot{\gamma}$, shear rate and R, droplet radius. The meaning of the k-term is a balance between the resistance to deformation of the droplet (σ/R) and the local acting shear stress ($\eta_m \dot{\gamma}$) that causes the droplet deformation. For the polymers of viscoelastic rather than of viscous nature, σ in the k-term has to be corrected by a factor that considers the effect of the normal forces arising from the elasticity of the phases. A theoretical model for viscosity

* Corresponding author. Fax: +86-28-85405402.
E-mail address: fuqiang1963@yahoo.com (Q. Fu).

0032-3861/03/$ - see front matter Published by Elsevier Ltd.
doi:10.1016/S0032-3861(03)00524-X

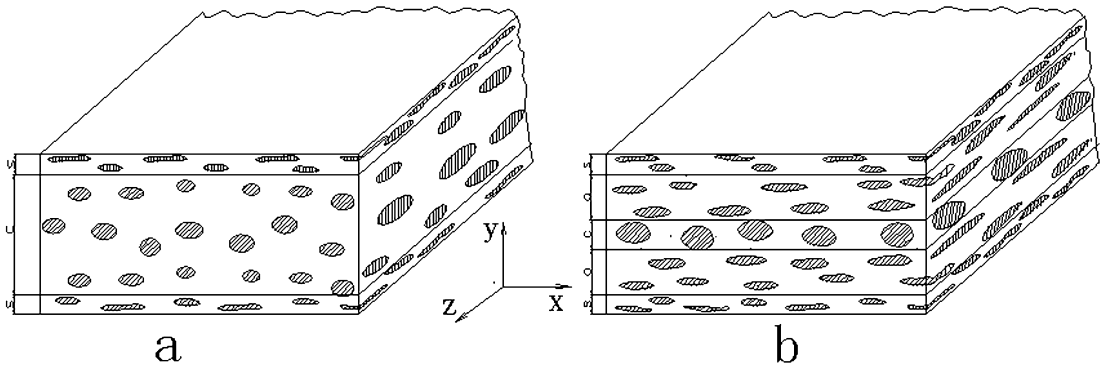

Fig. 1. the schematic diagram of morphology in various layers of both (a) static and (b) dynamic specimens, in which s is skin layer, o is oriented layer and c is core layer. In the coordinate system, x is the width of specimen, y is the thickness of specimen and z is the flow direction.

estimation of blends of stratified morphology has been proposed [12]. The transitions between droplets and stratified morphologies require a change in the melt elasticity ratio of the components. However, once the shear stress stops, the minor phase will relax and cause the deformed droplets to recover. Only if the morphology in the flow field is quenched instantaneously can the fibril or stratified morphology, that is only stable in flow, be preserved [13]. For instance, during the injection molding with higher injection speed, the skin layer, in close contact with the mold, quenches first. The minor phase morphology in this layer is frozen almost instantaneously. Thus, contact with the mold surface locally hinders the fibril disintegration and coalescence that takes place in the core, where the appearance of the spherical droplets may be attributed either to the elastic recovery and/or to the breaking up of the fibrils. Therefore, the minor phase morphology of this essentially quenched layer is very different from that of the core of the injection molded blends. Recently, in our group, during the stage of packing molding when the melt is injected into the cavity, the shear stress has been introduced by means of hydraulically actuated pistons [14,15]. Instead of the skin and core-like structure as seen in the samples injected by the traditional way, a morphology of core in the center and oriented zone surrounding the core and the skin layer is observed for the dynamic samples [16,17]. We have investigated the phase morphology and the deformation of dispersed particles in PP/EPDM blends [16], and the elongated rubber particles have been observed.

In previous work [17], super HDPE/EVA blends having high modulus (1.9–2.2 GPa), high tensile strength (100–120 MPa) and high impact strength (six times as that of pure HDPE) have been prepared by controlling the phase separation, molecular orientation and crystal morphology of the blends. The enhancement of tensile strength and modulus was believed to originate from the formation of the oriented layer, while the high impact strength was considered to be related to shear induced phase morphology. However, in the previous works, only the mechanical properties along shear flow direction were measured because a dumbbell specimen was used. For an oriented sample, the mechanical properties and morphology in both parallel and perpendicular to the shear flow direction should be measured. In order to investigate the effect of mechanical properties and phase morphology in the direction of orientation, in this paper, a square specimen was used. We have carried out a systematic investigation on the formation of phase morphology in HDPE/EVA blends under the effect of shear stress. In order to elucidate the difference of morphology in various layers of both dynamic and static specimens, a schematic representation is shown in Fig. 1.

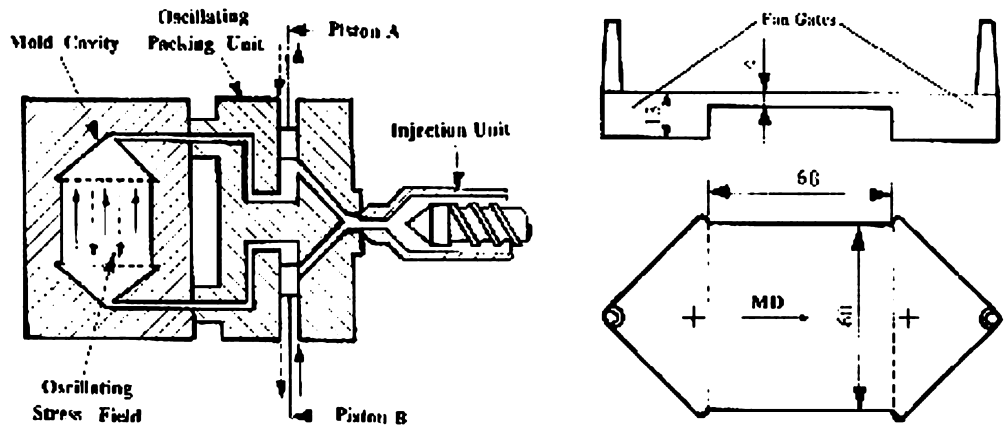

Fig. 2. The schematic representation of dynamic packing injection molding.

Table 1
Material used in the investigation

	Trade name	Characteristics			Producer
HDPE	2200J	MFI = 5.8	$d = 0.968$		Yansan Petrochemical Corp.
16EVA	630	MFI = 1.5	$d = 0.936$	VA% = 16	Toyo Soda Manufacturing Co., Ltd
33EVA	MB11	MFI = 45	$d = 0.960$	VA% = 33	Sumitomo Chemical Co., Ltd

Obviously, the shear imposes a significant effect on the morphology of the dynamic specimen (with shearing) and forms the so-called skin-oriented layer-core texture. This is totally different from the static specimen (without shearing) whose morphology consists of skin and core layer. The morphological difference at different layers is obvious and needs to be carefully investigated. However, due to the complicated skin-oriented layer-core morphology of the dynamic specimen, we cannot go into detail to discuss the phase morphologies at each layer for each composition. In this work, only the phase morphology formed in the oriented layer of the dynamic specimen is investigated to see the effect of shear stress and also for simplicity. The morphology at the same place in the core layer of the static specimen has also been investigated for comparison. The phase morphology in different directions (viewed along the shear flow or perpendicular to the flow direction) was checked to get an overall three-dimensional picture of phase morphology. The effect of viscosity ratio, interfacial tension, volume ratio and shear stress on the final morphology was discussed.

2. Experimental

2.1. Materials

The HDPE and EVAs, used in the experiment, are all commercialized products, and are summarized in Table 1. Two kinds of EVA were used with VA content 16 wt% (16EVA) and 33 wt% (33EVA), respectively. The melt flow index of EVA increases with VA content.

2.2. Samples preparation

Melt blending of HDPE/EVA was conducted using a TSSJ-25 co-rotating twin-screw extruder set at a barrel temperature of 160–190 °C. After making droplets, the blends were injected into a $68 \times 60 \times 4$ mm^3 mold, using a SZ 100 g injection molding machine set at 180 °C and 900 kg cm^{-2}. During the cooling, dynamic packing injection molding technology was applied, which relies on the application of shear stress fields to melt/solid interfaces during the packing stage by means of hydraulically actuated pistons. The maximum shear rate was 10–30 s^{-1}. The schematic representation of this technology is shown in Fig. 2. The detailed experimental procedures and the experimental devices were described in Ref. [14]. The processing parameters are listed in Table 2. Injection molding under static packing by using the same processing parameters was also carried out for comparison.

Table 2
Processing parameters in oscillating packing injection molding of HDPE/EVA blends

Parameters	Values
Injection pressure (MPa)	90
Oscillating packing pressure (MPa)	4
Oscillating frequency (Hz)	0.3
Holding time (min)	2
Melt temperature (°C)	180
Mold temperature (°C)	40

2.3. Scanning electron microscope

The phase morphology of HDPE/EVA blends was studied with an X-650 Hitachi scanning electron microscope at 20 kV. The specimens were fractured in liquid nitrogen, then preferentially etched in benzene. The etching process was allowed to continue for 24 hours at about 40 °C to reach the equilibrium condition. The solvent was removed from the specimen later using vacuum extraction. The surface was then coated with gold and subsequently examined.

3. Results

3.1. Phase morphology under the quiescent state

Fig. 3 shows the scanning electron microscope (SEM) photographs of fractured surface perpendicular to the flow direction of static samples of HDPE/33EVA blends with 33EVA content from 10 to 40 wt%. The black domains indicate the position of the extracted EVA phase. One observes a sea–island structure in the composition investigated up to 30 wt% of 33EVA, which indicates that EVA forms a dispersed phase and HDPE forms a continuous phase in these composition ranges. A co-continuous like morphology is seen at 40 wt% of 33EVA. The shape of EVA dispersed phase is spherical with a size of 0.5–1.0 μm when 33EVA content is no more than 20 wt%. However, as the 33EVA content reaches 30 wt%, the rubber particles become slightly elongated and the irregular rubber particles with a much larger size are seen at 40 wt% of 33EVA. For

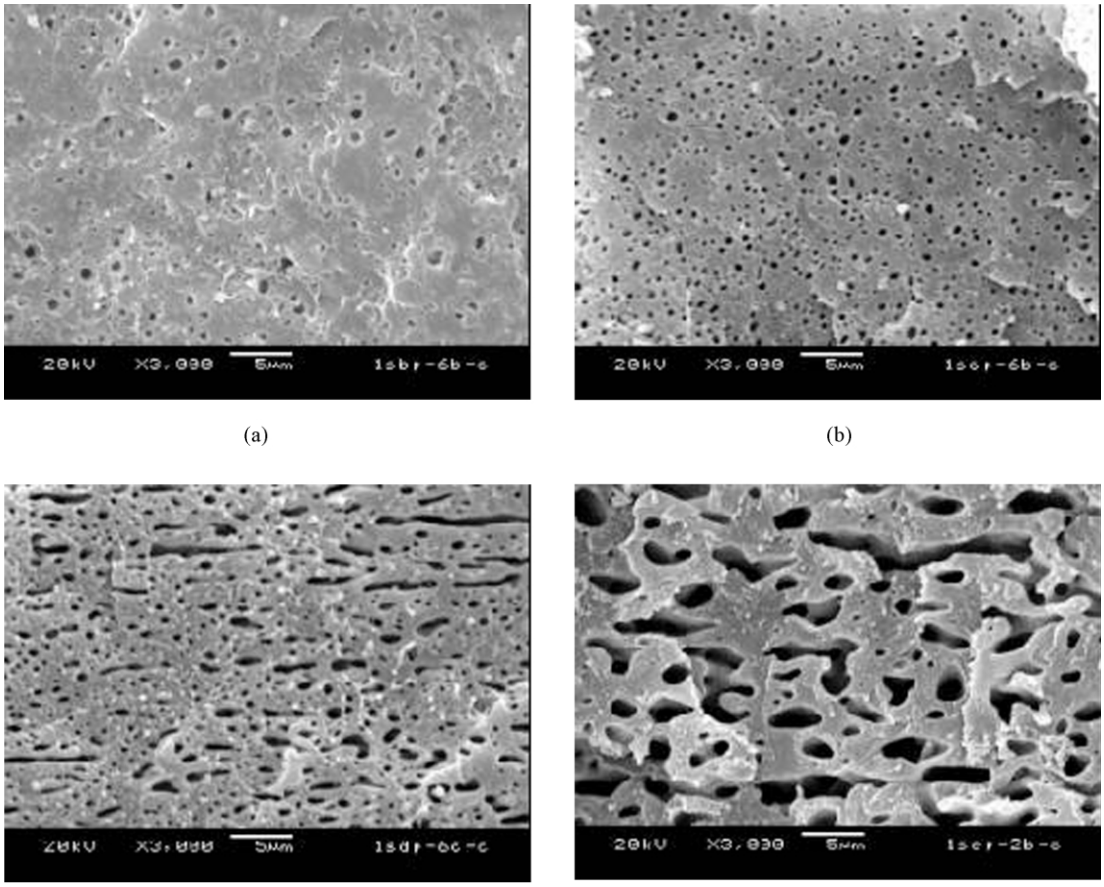

Fig. 3. SEM photographs of fractured surface perpendicular to the flow direction of static samples of HDPE/33EVA blends. HDPE/33EVA is (a) 90/10, (b) 80/20, (c) 70/30, and (d) 60/40.

comparison, the phase morphology along the flow direction is also examined. Compared with the morphology viewed perpendicular to the flow direction, much more elongated particles (at low EVA content) and even highly oriented layer morphology (at high EVA content) are seen, as expected. The SEM pictures of the fractured surface of HDPE/33EVA = 80/20 and 60/40 are shown in Fig. 4, as examples of phase morphology along flow direction. Instead of a co-continuous like structure, one observes a parallel layer structure. So one must be very careful to deal with the morphology having

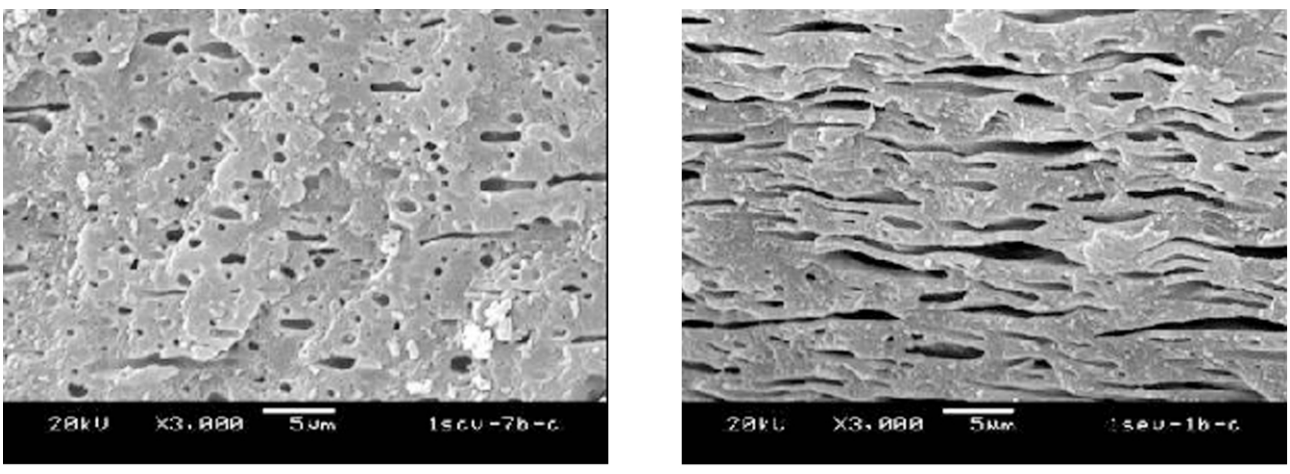

Fig. 4. SEM pictures of fractured surface of static samples of HDPE/33EVA blends along the flow direction. HDPE/33EVA is (a) 80/20 and (b) 60/40.

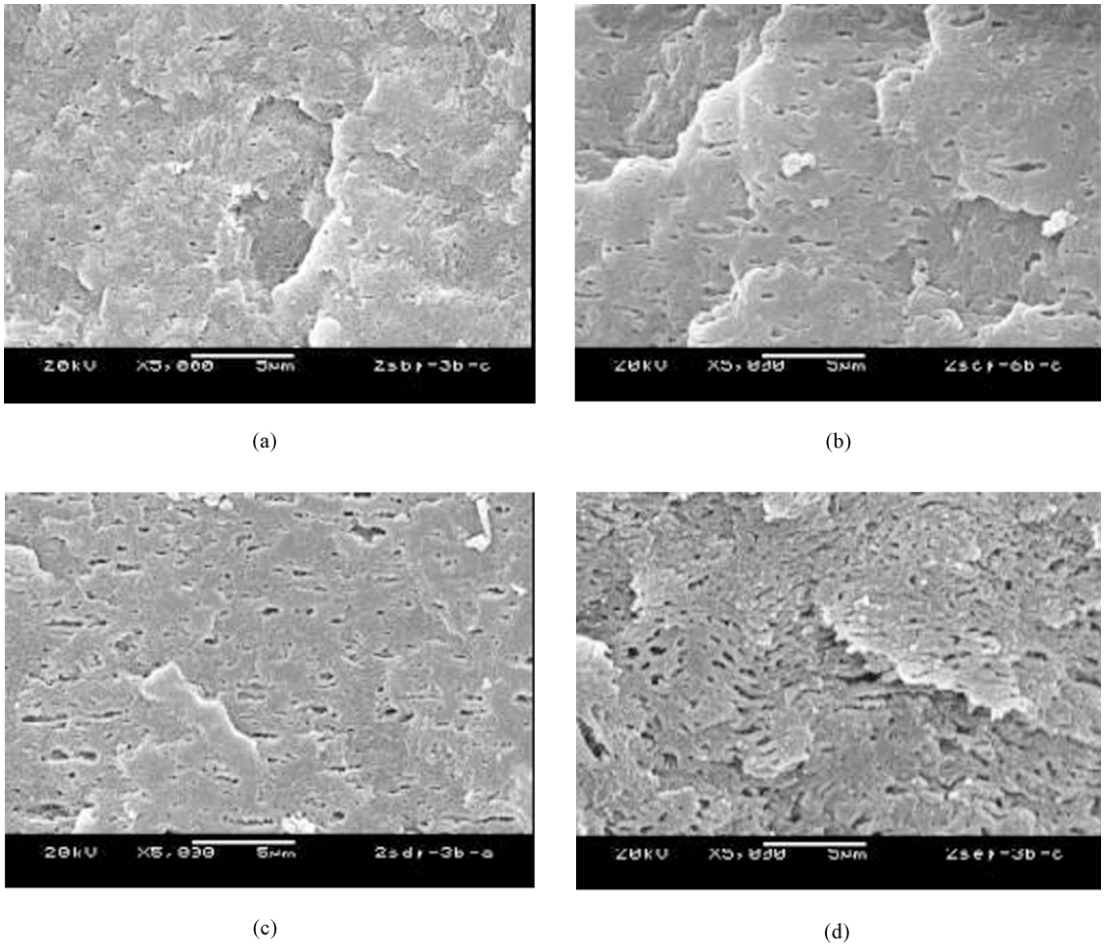

Fig. 5. SEM photographs of fractured surface perpendicular to the flow direction of static samples of HDPE/16EVA blends. HDPE/16EVA is (a) 90/10, (b) 80/20, (c) 70/30, and (d) 60/40.

anisotropic property. The morphologies viewed in different directions are needed to get the overall three-dimensional picture.

Fig. 5 shows the SEM photographs of fractured surface perpendicular to the flow direction of static samples of HDPE/16EVA blends with 16EVA content from 10 to 40 wt%. Compared with HDPE/33EVA blends, much smaller rubber particles (0.2–0.5 μm) are present, due to the better interaction between these two components. It should be noted that no phase inversion (co-continuous phase) is seen in the composition range investigated. Again the morphology along the flow direction is shown in Fig. 6. One observes a very similar morphology as in Fig. 5, and no remarkable deformation of particles is seen even along the flow direction. This may be attributed to the small size of rubber particles and/or better interfacial interaction. The elastic recovery may also play a role in this case due to the higher modulus of 16EVA compared with that of 33EVA.

Combined with the phase morphology parallel to the flow direction and perpendicular to the flow direction together, the three-dimensional phase morphology can be built up. The morphologies of static samples as a function of EVA content are schematically shown in Fig. 7. For HDPE/16EVA blends, only droplet morphology is formed as 16EVA content increases from10 to 40 wt%. However, for HDPE/33EVA blends, not only droplet, but also cylinder and co-continuous morphology (perpendicular to flow direction) can be formed depending on the volume ratio.

3.2. Phase morphology under low shear stress

The SEM pictures of fractured surface of HDPE/33EVA = 70/30 and 60/40 are shown in Fig. 8, as examples of phase morphology of dynamic samples viewed perpendicular to the flow direction. Very similar morphologies are seen as shown in Fig. 3(c) and (d) for static samples viewed perpendicular to the flow direction. Here again one observes slightly elongated particles at 30 wt% 33EVA content and a co-continuous like structure at 40 wt% 33EVA content. For dynamic samples, however, one is concerned much more with the morphology viewed along the flow direction where the effect of shear stress is mostly demonstrated. Fig. 9 shows the morphological development of HDPE/33EVA blends along the flow direction as a function of 33EVA content under shear stress. It can be seen that the shape of particles become

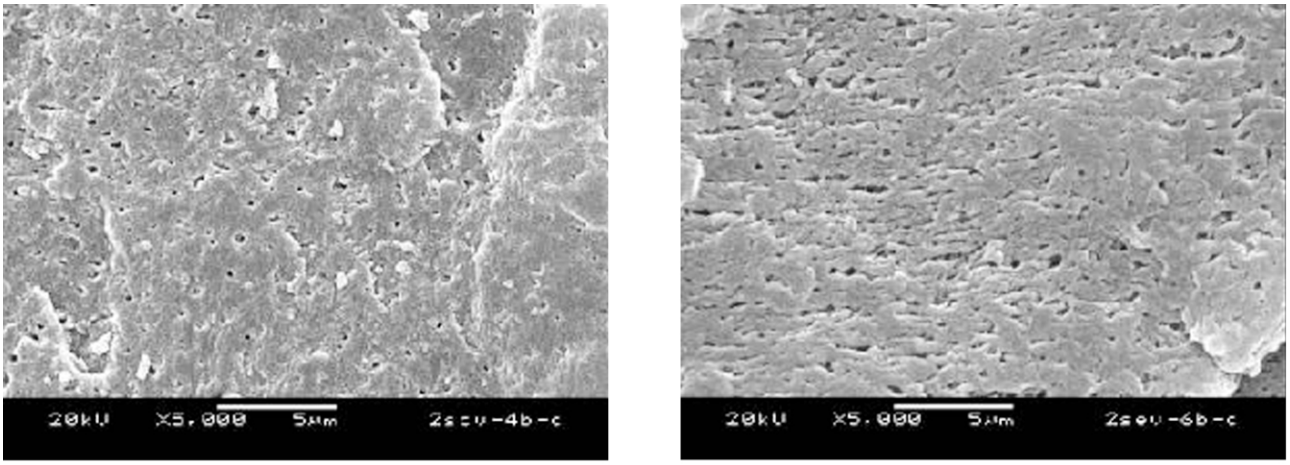

(a) (b)

Fig. 6. SEM pictures of fractured surface of static samples of HDPE/16EVA blends along the flow direction. HDPE/16EVA is (a) 80/20 and (b) 60/40.

much more elongated with increasing 33EVA content. A big jump of particle size and a co-continuous-like morphology occurs at 40 wt% of 33EVA content. So different from the static sample with 40 wt% 33EVA content, where a co-continuous-like morphology is seen only in the direction perpendicular to the flow direction, for a dynamic sample with the same composition, a co-continuous like morphology is observed both parallel and perpendicular to flow direction under the effect of shear stress.

For HDPE/16EVA blends, droplet morphology is formed at low 16EVA content, but much-elongated particles are seen at a high 16EVA content along the flow direction for dynamic samples, as shown in Fig. 10. One observes a layer-like structure for HDPE/16EVA = 70/30 and 60/40 blends due to high orientation of particles along the flow direction under the effect of shear stress. However, the thickness of the layer is much smaller than the layer formed in HDPE/33EAV blends. Fig. 11 shows the morphological development of HDPE/16EVA blends perpendicular to the flow direction as a function of 16EVA content for dynamic samples. A droplet-morphology with constant particle size is seen for all the compositions studied (16EVA content changes from 20 to 40 wt%).

In summary, combined with the phase morphology parallel to the flow direction and perpendicular to the flow direction together, the three-dimensional morphologies of

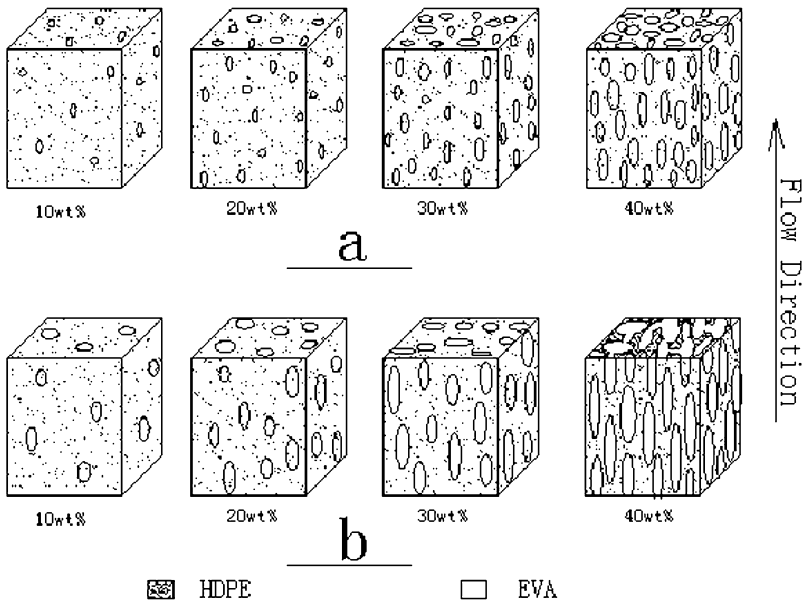

Fig. 7. The schematic representation of three-dimensional morphology of static samples, (a) HDPE/16EVA blends and (b) HDPE/33EVA blends.

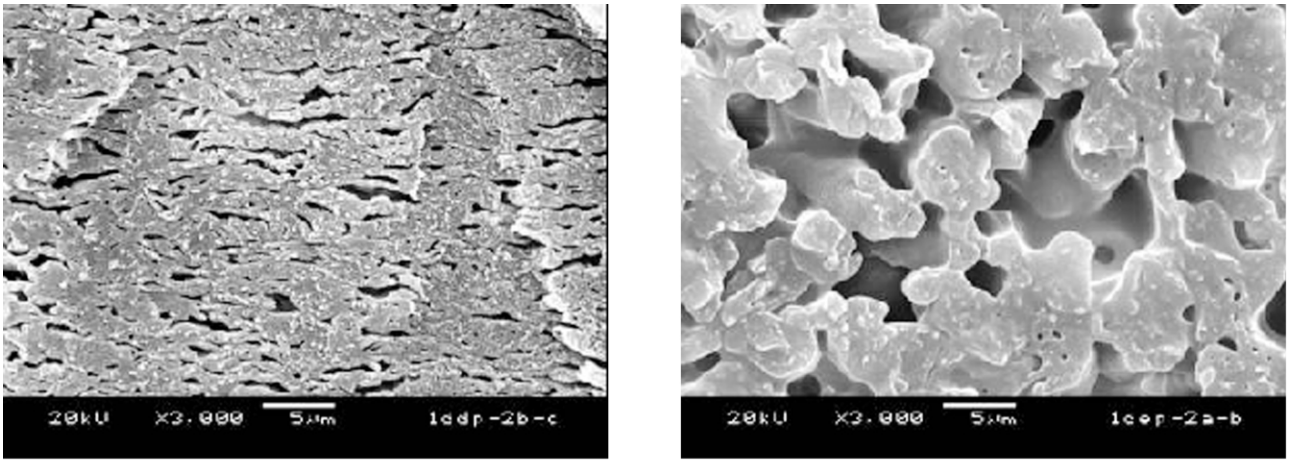

(a) (b)

Fig. 8. The SEM pictures of fractured surface perpendicular to the flow direction of dynamic samples of HDPE/33EVA is (a) 70/30 and (b) 60/40.

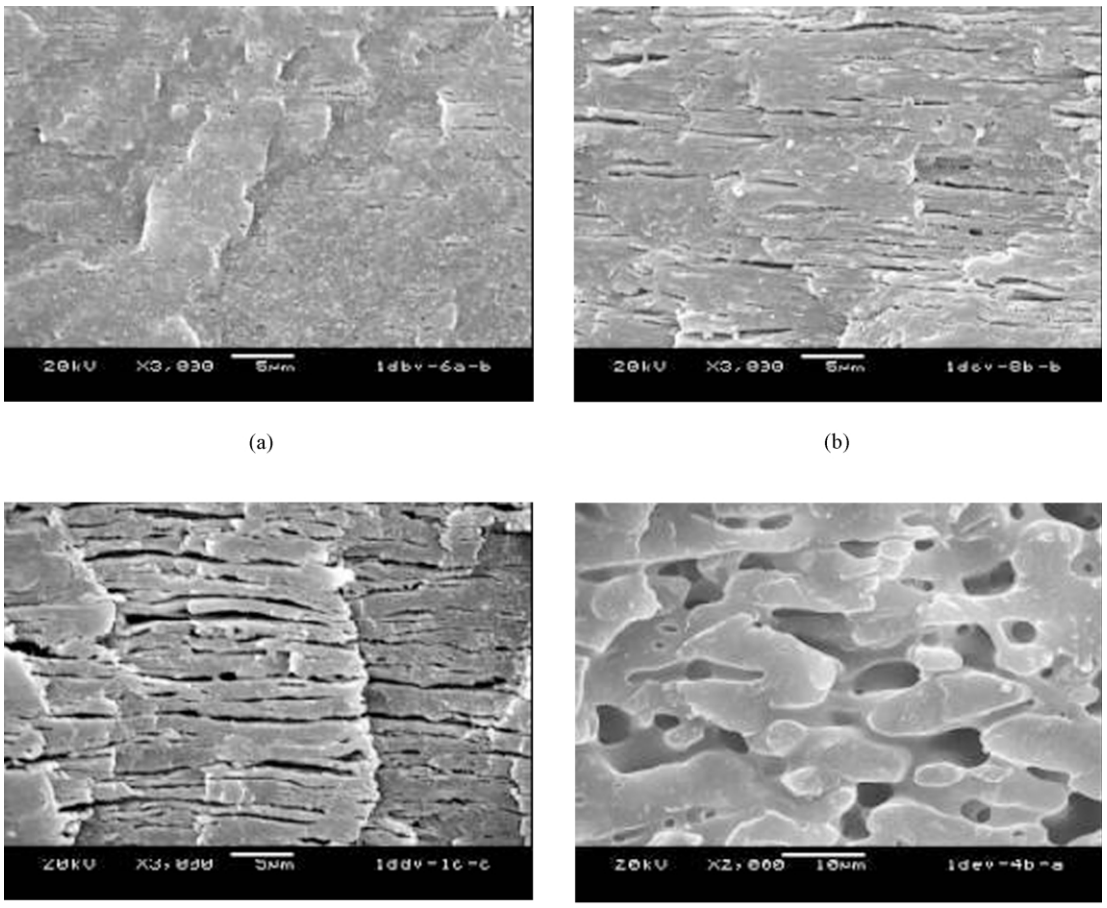

(a) (b)

(c) (d)

Fig. 9. SEM photographs of fractured surface along the flow direction of dynamic samples of HDPE/33EVA blends. HDPE/33EVA is (a) 90/10, (b) 80/20, (c) 70/30, and (d) 60/40.

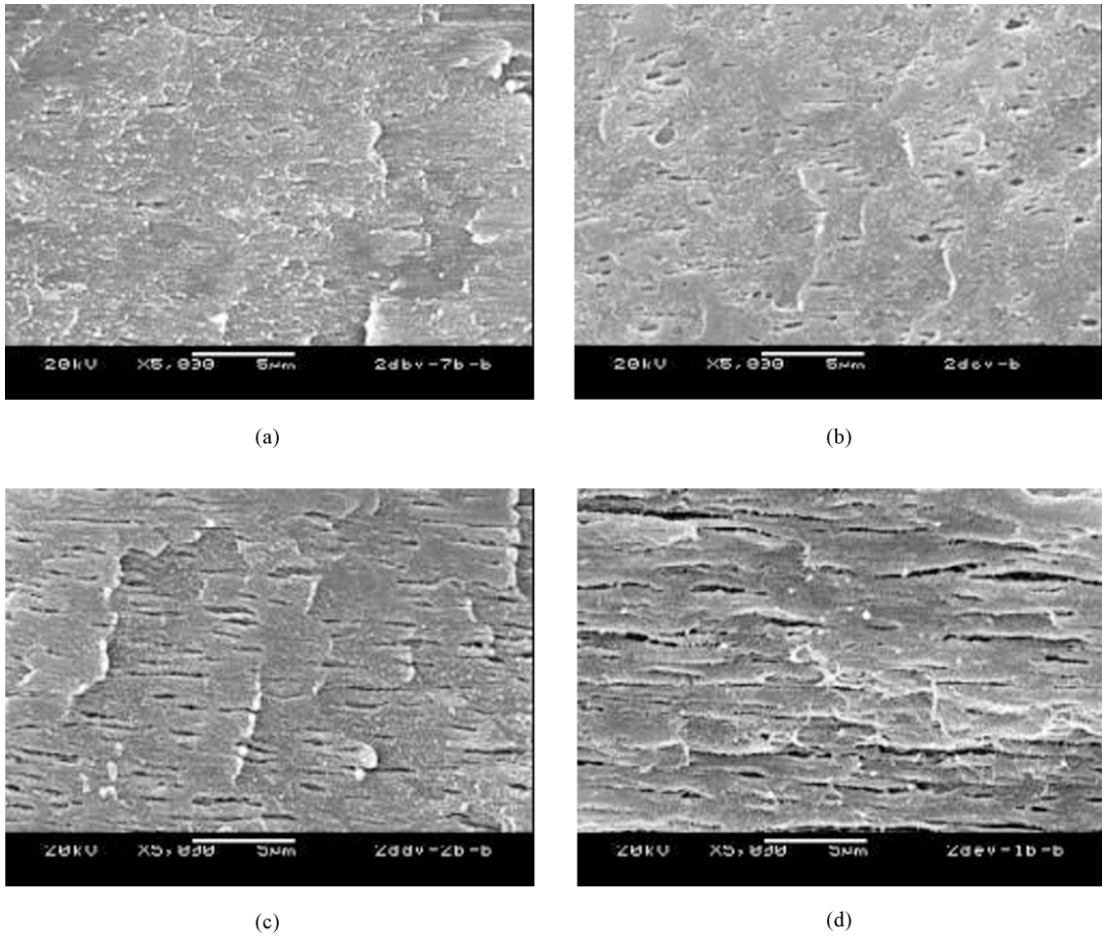

Fig. 10. SEM photographs of fractured surface along the flow direction of dynamic samples of HDPE/16EVA blends. HDPE/16EVA is (a) 90/10, (b) 80/20, (c) 70/30, and (d) 60/40.

dynamic samples, as a function of EVA content are schematically shown in Fig. 12. For HDPE/16EVA blends, both droplet and cylinder morphologies can be formed depending on the volume ratio. For HDPE/33EVA blends, droplet, cylinder and co-continuous network (co-continuous both in parallel and perpendicular to flow direction) can be formed under the effect of shear stress.

4. Discussions

4.1. The effect of viscosity ratio λ and k-term

In the steady shear flow, a purely viscous spherical droplet surrounded by another Newtonian fluid will be deformed to ellipse [18], which is shown in Fig. 13. Theoretical calculation and experimental observations have proven that its deformation is dominated by the cooperative effect of viscosity ratio λ and k-term [19,20] and the orientation angle of droplets in the shear flow field can be characterized by the equation as follows:

$$\theta = \frac{\pi}{4} + \frac{1}{2}\tan^{-1}(19\lambda/40k) \tag{3}$$

where θ, the angle between velocity gradient and the major axis of ellipse, which is also indicated in Fig. 13. According to the Eq. (3), Vanoene [10] has proposed that while $k \gg \lambda$, the major axis of droplets is oblique to the flow direction and this can illustrate that the factor of interfacial tension is dominated. Instead, while $\lambda \gg k$, the major axis of droplets is parallel to flow direction, which indicates that the factor of viscosity is dominated. In our case, from these SEM photographs, for every composition the rubber particles are all elongated along the flow direction. Therefore, it can be concluded that in the low shear stress field it is the factor of viscosity rather than the factor of interfacial tension that dominate the deformation along the flow direction.

Therefore, in this case, the contribution of interfacial tension to the deformation of droplets along the flow direction may only act through the change in the size of rubber particles. The effect of interfacial tension on the phase morphology is demonstrated by a substantial reduction in particle size in HDPE/16EVA blends. The reduced particle size is understood as resulting from the reduced interfacial tension. According to Eq. (2), the smaller the droplets, the greater is the resistance to deformation. So one always observes less deformed

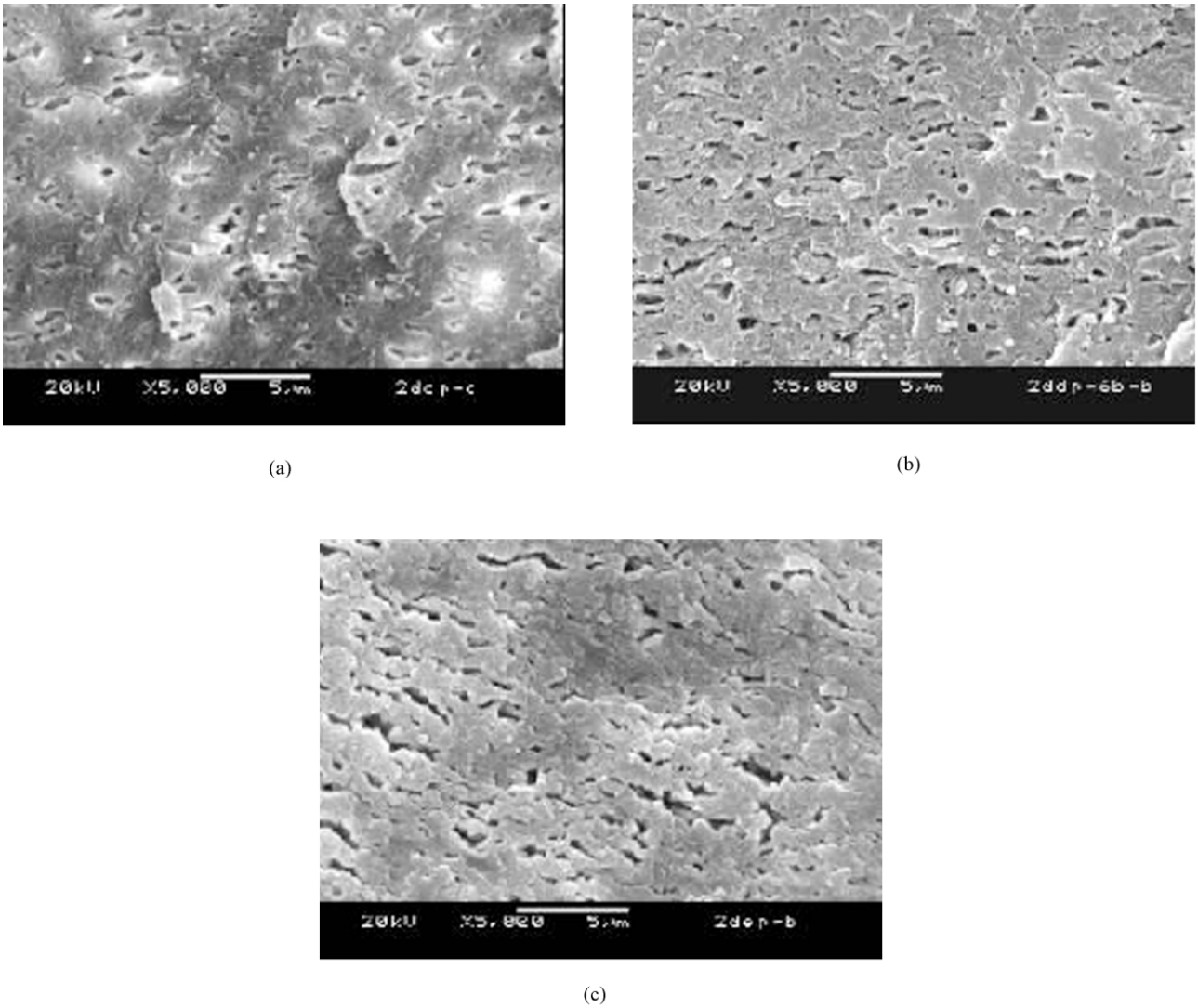

Fig. 11. The SEM pictures of fractured surface perpendicular to the flow direction of dynamic samples of HDPE/16EVA is (a) 80/20, (b) 70/30, and (c) 60/40.

particles in HDPE/16EVA blends. Of course, the elastic recovery may also play a role in this case due to the higher modulus of 16EVA compared with that of 33EVA. The effect of elastic recovery could be understood from the Rayleigh–Taylor–Tomotika theory [18,21] and the experimental observation was also found from Karger–Kocsis's work [22]

Furthermore, the viscosity ratio will also affect the deformation of rubber particles, as predicted by Eq. (1). The melt viscosity of the three materials (HDPE, 16EVA, and 33EVA) as a function of shear rate is measured by using a high-pressure capillary rheometer Rheograph 2002 (Gottfert) with a 1 mm die and *L*/*D* ratio of 30 at 180 °C over a shear rate range, $\dot{\gamma}$, from 10^1 to 10^4 s^{-1} and is shown in Fig. 14. Clearly, in the whole shear rate rank, the viscosity of 16EVA is the highest, and that of HDPE sets in the middle, and that of 33EVA is the lowest. Considering the high pressure injection molding and low pressure packing, the viscosity ratios were determined at 180 °C for the shear rate of 10 and 30 s^{-1}, respectively (see Table 3). For HDPE/33EVA blends, as the elasticity of the low viscosity of 33EVA is smaller than that of the HDPE, interfacial tension σ is reduced under shear stress, according to Oene [23], resulting in pronounced deformability. For HDPE/16EVA blends, due to the higher viscosity of 16EVA and its better

Table 3
The phase inversion of HDPE/EVA blend calculated from viscosity ratio

		Viscosity ratio (HDPE matrix) λ	Phase inversion (volume fraction of EVA)	
			Eq. (4)	Eq. (5)
16EVA	10 s^{-1}	2.1	0.68	0.6
	30 s^{-1}	1.8	0.64	0.59
33EVA	10 s^{-1}	0.23	0.19	0.35
	30 s^{-1}	0.25	0.20	0.35

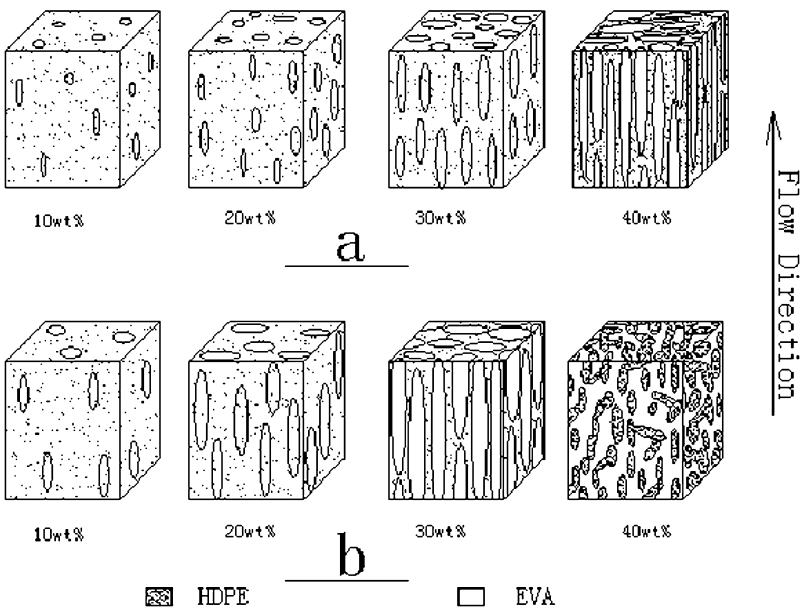

Fig. 12. The schematic representation of three-dimensional morphology of dynamic samples, (a) HDPE/16EVA blends and (b) HDPE/33EVA blends.

interaction with the HDPE, stabilization of the initial spherical droplet shape and less deformed particles are expected. It should be noted that the effect of reduced interfacial tension is twofold; it makes the droplets smaller on one hand, and also makes them more deformable on the other hand.

4.2. The effect of shear stress and region of phase inversion

As discussed above, for injection molded HDPE/EVA blends, the phase morphology is quite complicated. The effect of shear stress is evident from the anisotropy distribution of EVA size and the deformation of particles. The greater the shear stress, the easier is the deformation. Not only is this then in the deformation of particles, but also the shear induced phase separation at low shear rates are reported [24–26]. The effect of shear fields on phase behavior is theoretically interpreted in terms of the enhancement of concentration fluctuations and the elastic contribution to the free energy of mixing.

In the processing of polymer blends, with the increasing concentration of the minor phase, particles become close enough to behave as if they were connected. Further addition of minor phase material extends the continuity network until the minor phase is continuous throughout the sample. According to the percolation theory, the phase inversion occurs, which depends upon the viscosity ratio and composition. To estimate the point of phase inversion, the model proposed by Paul and Barlow [27] is:

$$\frac{\eta_1}{\eta_2}\frac{\phi_2}{\phi_1} = 1 \tag{4}$$

where ϕ_x is the volume fraction of x at phase inversion, and

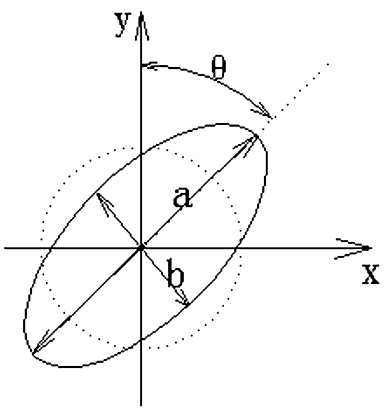

Fig. 13. The schematic diagram of droplet deformation in the shear flow, where a is the major axis and b is the minor axis of ellipse. In the coordinate system, x is the direction of shear flow, y is the velocity gradient, and θ is the orientation angle of droplet.

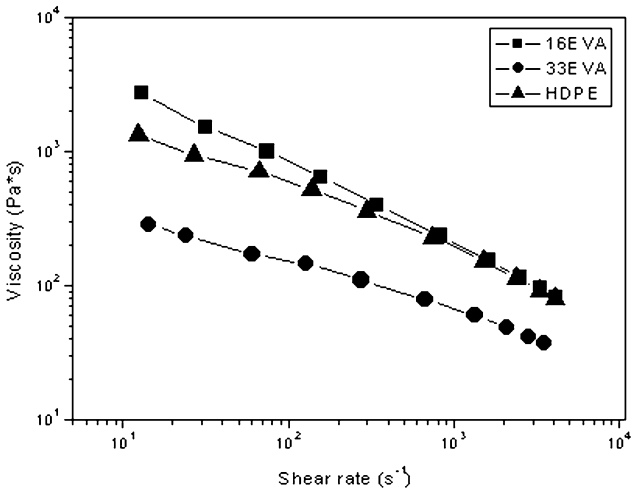

Fig. 14. The melt viscosity of HDPE, 16EVA and 33EVA at 180 °C as a function of shear rate.

η_x is the viscosity of phase. However, the equation does not always predict the region of phase inversion correctly, especially when blending material with a large difference in melt viscosity. Therefore, Chen and Su [28] have proposed an alternative equation:

$$\frac{\phi_{hv}}{\phi_{lv}} = 1.2\left(\frac{\eta_{hv}}{\eta_{lv}}\right)^{0.3} \quad (5)$$

where the subscripts 'hv' and 'lv' denote the high and the low viscosity phase, respectively. In order to calculate the viscosity ratio, λ, of the blend components for the applied processing conditions, capillary rheometry measurements were performed at the processing temperature of 180 °C. In general, shear rates for conventional large-scale injection equipment are situated in the orders of 10^2 s^{-1} [2]. And for our dynamic injection packing molding, during the stage of packing the shear rate added by the position is estimated to be in the order of 10^1 s^{-1}. From Fig. 14 and Table 3, one can easily predict the region of phase inversion via Eqs. (4) and (5), and the result is also listed in Table 3. It is pronounced that the region of phase inversion for HDPE/16EVA and HDPE/33EVA blends is approximately 0.60–0.65 and 0.35–0.40 of EVA, respectively. The data from Eq. (5) fits well with the experimental observation. Under the combined effect of shear stress and low viscosity ratio between HDPE and 33EVA, the co-continuous phase is also seen along the flow direction under the effect of shear stress at 40 wt% of 33EVA content.

5. Conclusion

Three-dimensional phase morphology of HDPE/EVA blends has been obtained. The shear stress, interfacial tension, viscosity ratio and volume ratio have great effect on the size of dispersed particles and the degree of deformation. Compared with the morphology viewed perpendicular to the flow direction, the phase morphology along the flow direction changes dramatically under the effect of shear stress. Generally, elongated and layer-like structures are formed along the flow direction, and spherical droplet-like morphology is formed perpendicular to the flow direction. For static samples of HDPE/16EVA blends (without shearing), only droplet morphology is formed as 16EAV content increases from10 to 40 wt%. However, for static samples of HDPE/33EVA blends, not only droplet, but also cylinder and co-continuous morphology (perpendicular to flow direction) can be formed depending on the volume ratio. For dynamic samples of HDPE/16EVA blends (under the effect of shear stress), both droplet and cylinder morphologies can be formed depending on the volume ratio. For dynamic samples of HDPE/33EVA blends, droplet, cylinder and co-continuous network (co-continuous both in parallel and perpendicular to flow direction) can be formed under the effect of shear stress.

Acknowledgements

We would like to express our great thanks to the China National Distinguished Young Investigator Fund, National Natural Science Foundation of China (No. 20274028) and the Research Fund for the Doctoral Program of Higher Education (No. 20020610004) for financial support.

References

[1] Utracki LA, Shi ZH. Polym Engng Sci 1992;32:1824.
[2] Wu S. Polym Engng Sci 1987;27:342.
[3] Sundararai U, Macosko CW. Macromolecules 1995;28:2647.
[4] Favis BD, Chalifoux JP. Polymer 1988;29:1761.
[5] Namhata S, Guest MJ, Aerts LM. J Appl Polym Sci 1999;71:311.
[6] Elmendorp JJ. In: Rauwendaal C, editor. Mixing in polymer processing. New York: Marcel-Dekker; 1991.
[7] Ghiam F, White JL. Polym Engng Sci 1991;31:76.
[8] Kamal MR, Song L, Singh P. Polym Compos 1986;7:323.
[9] Plochocki AP. Polym Engng Sci 1983;23:618.
[10] Vanoene H. J Colloid Interf Sci 1972;40:445.
[11] Elemendorp JJ. Polym Engng Sci 1986;26:418.
[12] Lin CC. Polym J 1979;11:185.
[13] Kamal MR, Sahto MA, Utracki LA. Polym Engng Sci 1983;23:637.
[14] Zhang G. PhD Thesis. Chengdu, China: Sichuan University; 2000.
[15] Guan Q, Lai FS, Shen KZ. Polymer 1997;38:5251.
[16] Wang Y, Li Q, Fu Q. Macromol Engng Mater 2002;287:391.
[17] Na B, Zhang Q, Fu Q. Polymer 2002;43:7367.
[18] Taylor GI. Proc R Soc London, Ser A 1934;146:501.
[19] Cox RG. J Fluid Mech 1969;37:601.
[20] Choi SJ, Schowaller WR. Phys Fluids 1975;18:420.
[21] Tomotika S. Proc R Soc London, Ser A 1935;150:322.
[22] Karger-Kocsis J, Csikai I. Polym Engng Sci 1987;27:241.
[23] Oene H. Yan. J Colloid Interf Sci 1972;40:448.
[24] Hindawi IA, Higgins JS, Weiss RA. Polymer 1992;33:2522.
[25] Katsaros JD, Malone MF, Winter HH. Polym Bull 1986;16:83.
[26] Hindawi IA, Higgins JS, Galambos AF, Weiss RA. Macromolecules 1990;23:670.
[27] Paul DR, Barlow JW. J Macromol Sci, Rev Macromol Chem Phys 1980;C18:109.
[28] Chen TH, Su AC. Polymer 1993;34:4826.